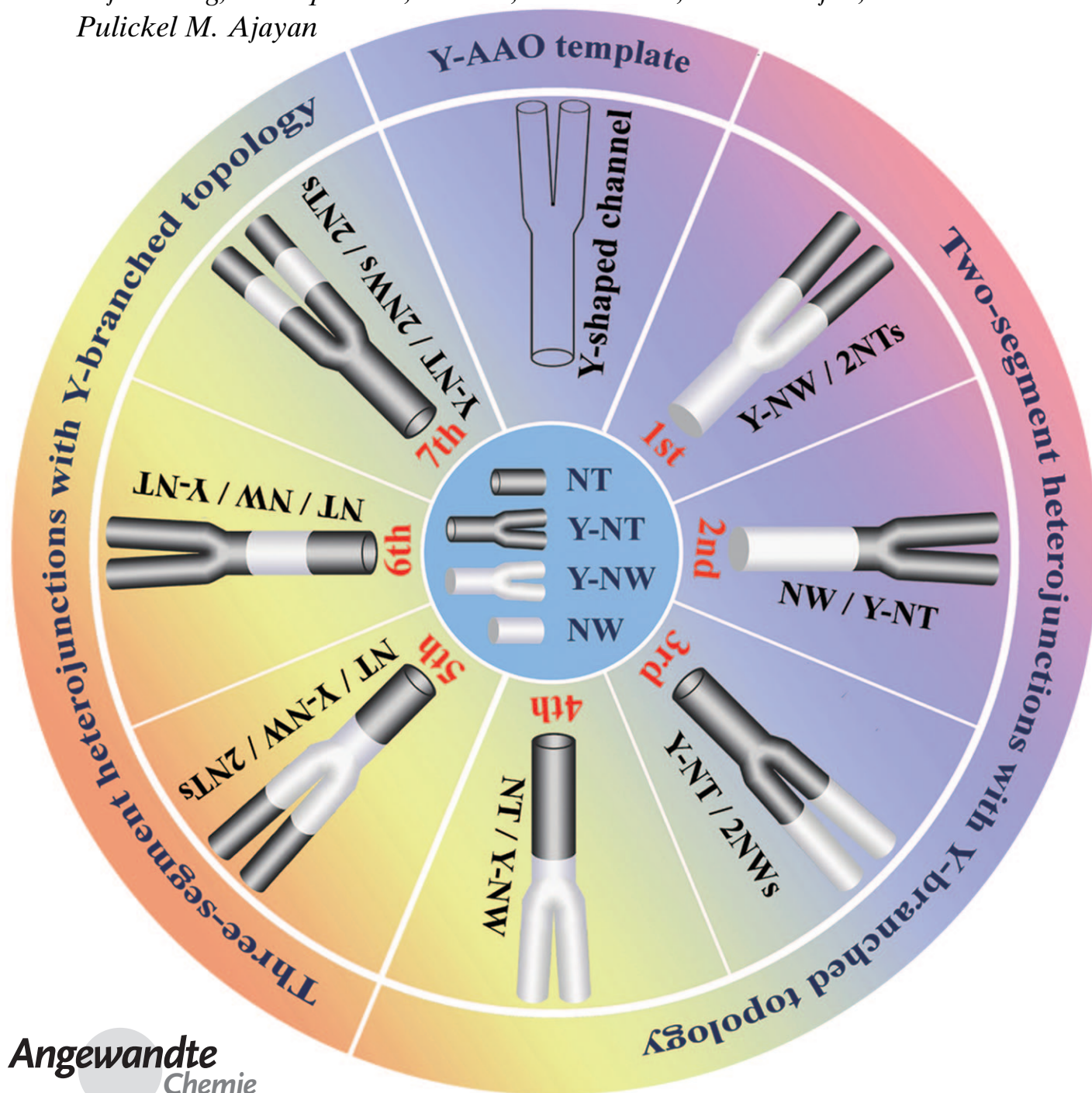


A General Synthetic Approach to Interconnected Nanowire/Nanotube and Nanotube/Nanowire/Nanotube Heterojunctions with Branched Topology**

Guowen Meng,* Fangming Han, Xianglong Zhao, Bensong Chen, Dachi Yang, Jianxiong Liu, Qiaoling Xu, Mingguang Kong, Xiaoguang Zhu, Yung Joon Jung, Yajun Yang, Zhaoqin Chu, Min Ye, Swastik Kar, Robert Vajtai, and Pulickel M. Ajayan



Heterojunctions between nanotubes (NTs) and nanowires (NWs) could provide building blocks for nanoelectronics and nanophotonics,^[1,2] with other applications in barcodes,^[3] optical readout,^[4] biomolecular separation,^[5] catalysis,^[6] self-assembly,^[7] and magnetic manipulation.^[8] Although hybrid NWs (metal/polymer,^[7] semiconductor/semiconductor,^[1,2,9] metal/semiconductor,^[10] and metal/metal^[3,4,8,11]), hybrid NTs (metal/metal),^[12] NT/NW heterojunctions,^[13] and tree-like nano-heterojunctions^[14,15] have been made, the corresponding studies demonstrated limited control over the geometry and complexity of the nano-heterojunctions, which ultimately are central to the design of building blocks for nanocircuits, nanodevices, and nanosystems. Herein we show a general synthetic approach to various branched two-segment NW/NT and three-segment NT/NW/NT heterojunctions, based on a combinatorial process of electrodepositing NWs within the branched channels of anodic aluminum oxide (AAO) templates,^[16,17] selectively etching part of the electrodeposited NWs, and growing NTs on the ends of the NWs. The NWs can be metallic or semiconducting, while the NTs can consist of carbon, silicon, and silica; the two NT segments in three-segment NT/NW/NT nanoarchitectures can comprise either the same or different materials. This approach enables excellent control over the geometry, chemical composition, and complexity of the hetero-nanoarchitectures that can be the framework for nanoscale devices and systems.

Figure 1 shows schematic depictions of the basic hetero-nanoarchitectures we have made, which consist of various NT and NW segments placed combinatorially in a Y-shaped topology. The synthesis scheme follows a typical building-block concept in which a set of different nanoscale components (NTs and NWs of different materials with distinct properties, in linear and branched topologies) can be connected in a predetermined fashion inside the branched

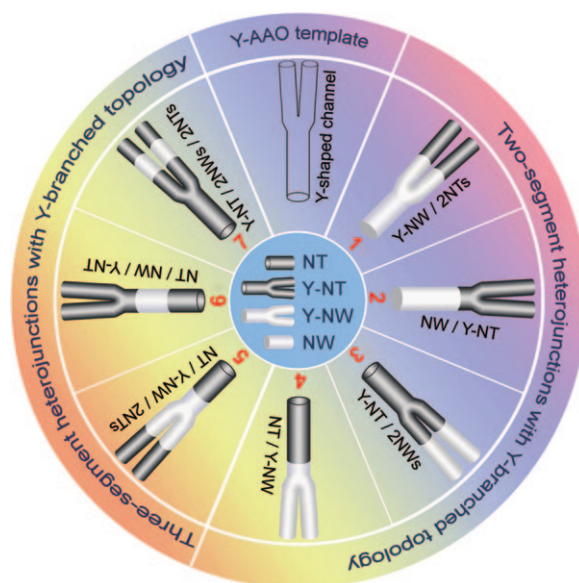


Figure 1. Schematic drawing showing a catalog of NT/NW and NT/NW/NT hybrid architectures with Y-branched topology. NTs (hollow) are shown in black and NWs (solid) in white; Y-NT and Y-NW indicate Y-shaped NTs and NWs. The eight fan-shaped sections show one of the Y-shaped channels and seven types of hybrid NT/NW and NT/NW/NT architectures. Each red number designates a given architecture. In the symbolic expressions (e.g. Y-NW/2NTs), the slash denotes the interface at the junction between NT and NW; 2NTs and 2NWs stand for two parallel NTs and NWs in the branches, respectively. The seven types of hybrid architectures with Y-shaped topology are categorized according to the number of hybrid segments in the axial direction: two segments (1–4; on the right) or three segments (5–7; on the left).

channels^[16,17] of the AAO template to produce objects that differ distinctly in architecture and functionality. We describe below the various synthetic steps that lead to the distinct architectures shown in Figure 1. While this approach can be easily extended to a wider variety of complex channel shapes (e.g. multiple generations of Y branching and multiple branchings from one stem),^[17] we demonstrate herein the Y-branched hybrid nanoarchitectures by using Y-shaped-channel AAO (Y-AAO) as the template. The diameters of the main stem and the branches are typically 80–90 and 55–65 nm, respectively.

One of the hybrid architectures we have produced has the NW segment occupying the Y-junction region, and the NTs (e.g. carbon NTs, CNTs) are part of the branches of the Y construct (architecture 1). This architecture can be made, as shown schematically in the top panels of Figure 2a, by coating the planar surface of the stem-channel side with a metallic layer as working electrode and then using electrochemical deposition (ECD) to form NWs of the designated material (e.g. nickel NWs, NiNWs) in the channels of the template. The duration of ECD is adjusted to fill the channels beyond the Y-junction level, leaving some empty space in the branched channels (Supporting Information, Figure S1). In the last step, chemical vapor deposition (CVD) is used to deposit CNTs^[16,17] in the spaces left empty after the previous step. The resultant Y-NiNW/2CNTs architecture is shown in the

[*] Prof. G. W. Meng, Dr. F. M. Han,^[†] Dr. X. L. Zhao,^[†] Dr. B. S. Chen, Dr. D. C. Yang, Prof. J. X. Liu, Dr. Q. L. Xu, M. G. Kong, X. G. Zhu, Dr. Y. J. Yang, Z. Q. Chu, M. Ye
Key Laboratory of Materials Physics and Anhui Key Laboratory of Nanomaterials and Nanostructures, Institute of Solid State Physics Chinese Academy of Sciences, Hefei, Anhui 230031 (China)
Fax: (+86) 551-559-1434
E-mail: gwmeng@issp.ac.cn

Prof. Y. J. Jung
Department of Mechanical & Industrial Engineering
Northeastern University, Boston, MA 02115 (USA)

Dr. S. Kar
Department of Physics, Applied Physics and Astronomy
Rensselaer Polytechnic Institute, Troy, NY 12180 (USA)

Dr. R. Vajtai, Prof. P. M. Ajayan
Department of Mechanical Engineering and Materials Science
Rice University, Houston, TX 77005 (USA)

[†] These authors contributed equally to this work.

[**] This work was supported by the National Science Fund for Distinguished Young Scholars of China (Grant No. 50525207), National Basic Research Program of China (Grant No. 2007CB936601), the Nanoscale Science and Engineering Initiative of the NSF under Award DMR-0117792, and NSF CMMI-0708541-NER.

Supporting information for this article is available on the WWW under <http://dx.doi.org/10.1002/anie.200901999>.

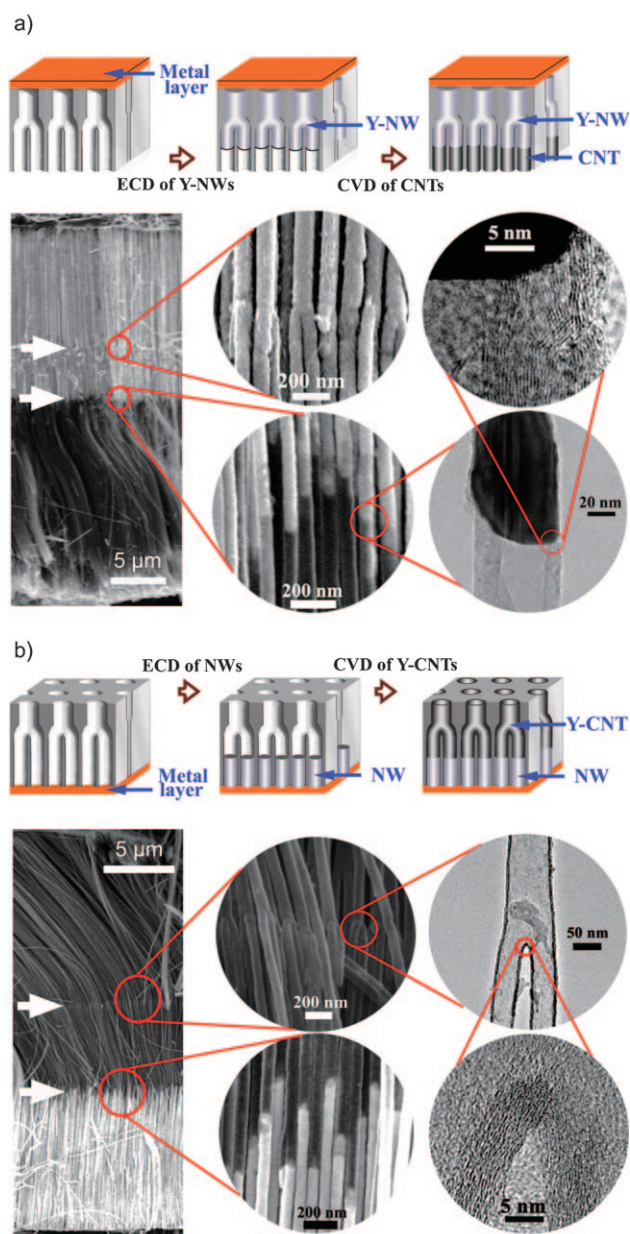


Figure 2. Two types of mirrored NT/NW hybrid architectures with Y-branched topology. a) Y-NiNW/2CNTs hybrid structure. One Y-shaped NiNW connects with two parallel CNTs in the branches of the Y construct. b) Y-CNT/2NiNWs hybrid structure. One Y-CNT connects with two parallel NiNWs in the branches of the Y construct. The upper panels are schematic drawings depicting three characteristic moments of the fabrication procedure, in which the planar surface of the stem-channel side (a) or branched-channel side (b) of the Y-AAO templates is coated with a thin metal layer as electrode in the ECD of NiNWs. The lower panels on the left are scanning electron microscopy (SEM) images of a bundle of the structures after template removal, in which the light and dark parts are NiNWs and CNTs, respectively; the two parallel interfaces (white arrows) show Y branchings and NiNW/CNT junctions. The lower middle panels are close-up views of the Y branchings (top) and NiNW/CNT junctions (bottom). The lower right panels are TEM (top) and high-resolution TEM images (bottom) of a NiNW/CNT junction (a) and a Y-CNT (b).

lower panels of Figure 2a. Energy-dispersive X-ray spectroscopy (EDS) measurements reveal the correct compositions of

the materials that have been deposited in sequence (Supporting Information, Figure S2). The enlarged SEM and TEM images reveal that the NiNWs are solid. Enlarged SEM views of the NiNW/CNT junction indicate that NiNWs and CNTs connected longitudinally in the branches have the same diameter, and the interface between the NiNW and the CNT is contiguous. Transmission electron microscopy (TEM) and high-resolution TEM images taken on a typical CNT/NiNW junction reveal that the interface is well-connected and that the CNT is multiwalled. With a little modification of the fabrication process, a different structure of NiNW/Y-CNT can be obtained (architecture 2). A shorter duration of electrodeposition results in NWs that do not reach the Y-junction region, which is then filled from the opposite side with Y-CNTs grown by CVD (Supporting Information, Figure S3, architecture 2 of NiNW/Y-CNT).

We also changed the ECD sequence; this time, the metal electrode is sputtered onto the planar surface of the branched-channel side. This approach allows the fabrication of a structure (architecture 3) mirroring the one in Figure 2a. Figure 2b depicts the architecture of Y-CNT/2NiNWs. There are shorter NiNWs in the branches (Supporting Information, Figure S4), and the rest of the structure consists of Y-CNTs. From the right panel of Figure 2b, it can be seen that the closely curved inner side of the Y-CNT is also graphitic in nature. This architecture is the exact reverse of 1 (Figure 2a), in which the NW and CNT segments have been interchanged. Longer NWs can also be grown with this configuration to result in NWs beyond the Y-junction level; subsequent CVD will add a CNT at the stem to achieve a different CNT/Y-NiNW structure (architecture 4, Supporting Information, Figure S5).

Further complexity in the architectures can be achieved by inserting one more NT segment on the other end of the NWs to achieve three-segment NT/NW/NT hybrid structures (architectures 5–7). For example, a hybrid structure of CNT/Y-NiNW/2CNTs (architecture 5) can be prepared, as shown schematically in Figure 3a. The metal electrode is first sputtered onto the planar surface of the stem-channel side, and NWs with Y junctions are subsequently electrodeposited. In the next step, the electrode metal and part of the neighboring NWs are removed by selective etching, leaving the Y junction of the NW intact but also providing empty space for NT deposition in the stem-channel (Supporting Information, Figure S6). The CVD step to fill the empty channels at both ends of the branches and the stems with CNTs completes the preparation process. The resulting CNT/Y-NiNW/2CNTs architecture is shown in Figure 3b, which displays a low-magnification SEM image of the structure and the three junctions: CNT/NiNW in the stem, Y junction in the Y-NiNW, and NiNW/CNT in the branches. The TEM image (lower left) of a representative Y-NiNW (selected area electron diffraction (SAED) pattern in the inset) shows the single-crystalline nature of the NiNW, which resulted from the high-temperature heating during CNT growth. The right panel shows a typical TEM image (top) of the CNT/NiNW junction located in the stem with a diameter of about 85 nm; the lower part is a lattice-resolved image taken from the area highlighted (circle) in the top image, revealing that the multiwalled CNT ends are close to the junction interface,

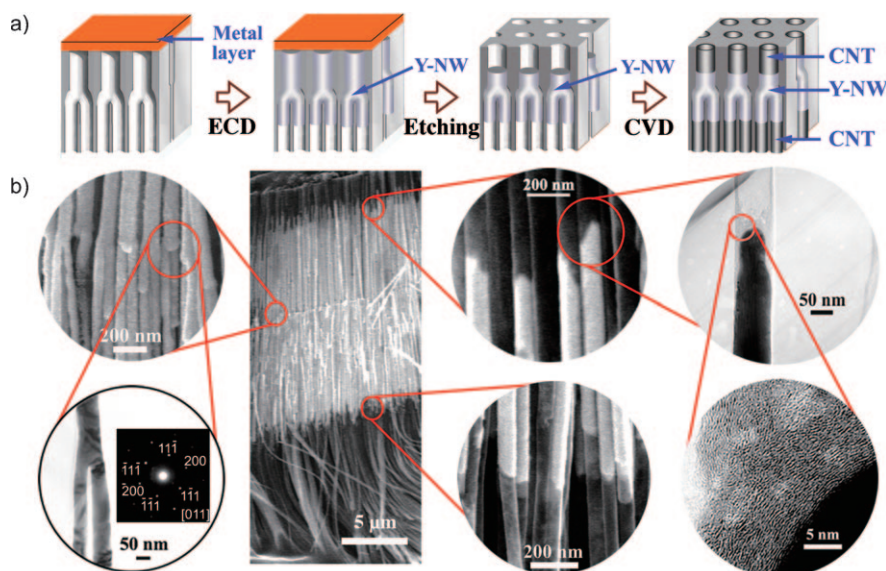


Figure 3. CNT/Y-NiNW/2CNTs hybrid architecture. One CNT connects with a Y-shaped NiNW and then connects with two CNTs in the branches of the Y construct. a) The fabrication procedure, in which the planar surface of the stem-channel side of the Y-AAO template is coated with a metal layer as electrode in the ECD of Y-NiNWs. b) The second panel from the left shows an SEM image of a bundle of the structures after template removal: the light part (in the middle) and the dark parts (top and bottom) are NiNWs and CNTs, respectively. The left panels show the Y branchings of the Y-NiNWs (top) and a TEM image of a single Y-NiNW (bottom, inset: the SAED pattern). The third panels from the left are close-up views of CNT/NiNW junctions in the stem (top) and the NiNW/CNT junctions in the branch (bottom). The right panels are TEM (top) and high-resolution TEM (bottom) images of a CNT/NiNW junction in the stem.

therefore good adherence between the NiNW and the CNT has been achieved. Modifications to the above approach can result in two other types of three-segment CNT/NW/CNT hybrid structures by positioning the NW segment away from the Y-junction area. In this way, architectures can be constructed in which the Y junction is located in the CNT segment and the NW segment is either in the middle of the stem (Supporting Information, Figure S7, architecture 6 of CNT/NiNW/Y-CNT) or in the middle of the branches (Supporting Information, Figure S8, architecture 7 of Y-CNT/2NiNWs/2CNTs).

Another possibility is to change the materials for both the NW and the NT segments; we have demonstrated hybrid nanostructures 1–7 with the magnetic metal nickel in the NW segment and CNTs in the NT segment. As for the NW segment, not only other metals (e.g. nonmagnetic copper) can be used to form the NW segment (Supporting Information, Figures S9 and S10 for CuNW/Y-CNT and Y-CNT/2CuNWs/2CNTs, respectively), but also a wide range of other materials can form the NW segment in the hybrid structures. These materials must be amenable to electrodeposition, be able to be selectively etched, and be stable under the growth conditions of the NTs. For example, Group II–VI compound semiconductors (Supporting Information, Figure S11, CNT/CdSNW/Y-CNT hybrid structure), magnetic alloys of CoPt (Supporting Information, Figure S12, Y-CNT/2CoPtNW/2CNT hybrid structure), and NiCo (Supporting Information, Figure S13, Y-CNT/2NiCoNW/2CNT hybrid structure) have been used to construct the NW segments. Even very stable

noble metals (e.g. Au) can be incorporated as the NW segment in the middle of the NT/NW/NT architectures by additional electrodeposition of a sacrificial segment of a different metal (e.g. Co) before electrodeposition of the desired noble-metal NW segment (Supporting Information, Figures S14 and S15, Y-CNT/2AuNW/2CNT structure). It should be noted further that the NW segment itself in the above hybrid structures could also consist of more than one subsegment comprising different materials with distinct properties. For example, two sub-NWs of magnetic Ni and nonmagnetic Ag have been constructed to yield a complete NW segment in Y-CNT/2AgNWs/2NiNWs/2CNTs (Supporting Information, Figures S16 and S17).

Furthermore, the CNT segments in the architectures can be replaced by NTs of other materials using appropriate growth techniques. As Si and SiO₂ can be incorporated in NTs inside the AAO template by CVD^[18] and repeated dipping,^[19] respectively, semiconducting SiNTs and insulating SiO₂NTs have been constructed in our architectures (Supporting Infor-

mation, Figures S18 and S19 for Y-SiNT/2AuNWs/2SiNTs and Figures S20 and S21 for Y-SiO₂NT/2AuNWs/2SiO₂NTs). Lastly, the two end NT segments in NT/NW/NT structures can comprise not only the same material (as all those demonstrated above) but also different materials. For example, a Y-SiNT/2AuNWs/2CNTs structure has been prepared, in which a polycrystalline Y-SiNT connects with two single-crystalline AuNWs and two CNTs in the branches in sequence (Figure 4 and Supporting Information, Figure S22).

By exploiting the demonstrated flexibility of our method for fabricating interconnected NT/NW and NT/NW/NT heteroarchitectures with Y-shaped topology, the complexity of the architectures may easily be extended further. The Y-branched topology can be extended to multibranch systems; for example, a three-branched hybrid architecture has been prepared (Supporting Information, Figure S23, three-branched-CNT/3NiNWs/3CNTs architecture). It is also possible to use AAO templates with channels of more complex shapes, that is, multiple generations of Y branching, or even the combination of Y branching with multibranches,^[17] to achieve NT/NW and NT/NW/NT hybrid architectures with more complex shapes.

In conclusion, a combinatorial process of electrodepositing NWs within the branched nanochannels of AAO template, selectively etching part of the deposited NWs, and growing NTs in the empty channels on the ends of the NWs, has been used to produce high yields of complex-shaped NT/NW and NT/NW/NT hybrid nanostructures with excellent control over the hierarchy, composition, and placement of the

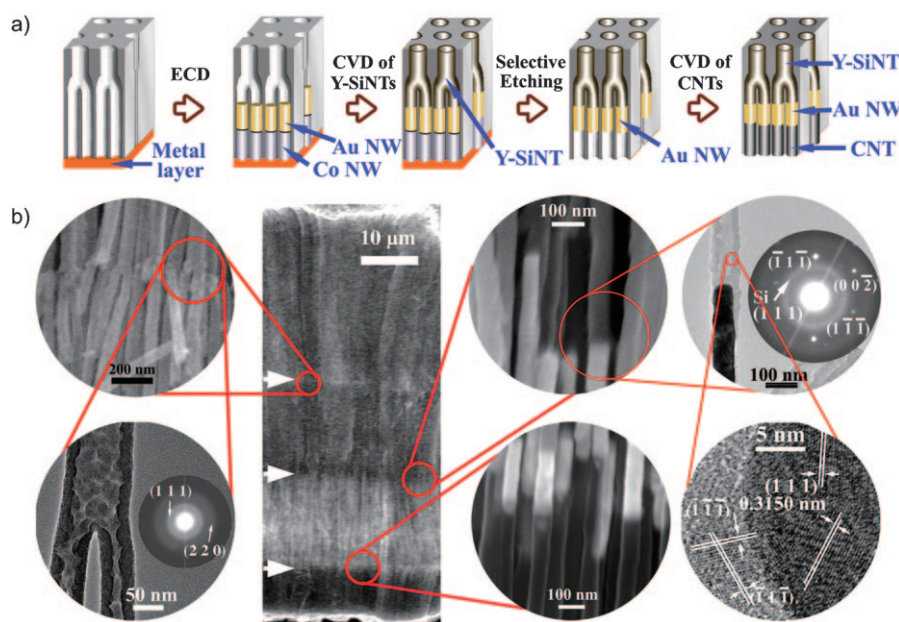


Figure 4. Y-SiNT/2AuNWs/2CNTs architecture. One Y-shaped SiNT linearly connects with two AuNWs and then with two CNTs in the branches in sequence. a) Consecutive stages of the fabrication procedure, in which first a sacrificial segment of CoNWs and then the desired AuNWs are electrodeposited in sequence. Second, Y-SiNTs are grown inside the empty top Y-shaped channels. Third, the metal electrode and the sacrificial CoNWs segment are etched away selectively, and finally CNTs are grown inside the bottom branched channels. b) The second panel from the left is a low-magnification SEM image of a bundle of the structures after template removal, in which the top medium contrast, the light contrast (in the middle near the bottom), and the bottom dark parts are SiNTs, AuNWs, and CNTs, respectively (Supporting Information, Figure S22). The three parallel interfaces (white arrows) show the interfaces of Y branches and of the two SiNT/AuNW and AuNW/CNT junctions. The left panels are an SEM image of Y-SiNTs (top) and a TEM image of a Y-SiNT (bottom; inset is the SAED pattern). The third panels from the left are close-up views of SiNT/AuNW (top) and AuNW/CNT (bottom) junctions. The right panels are TEM images of well-connected SiNT/AuNW junctions (top) with the SAED pattern from AuNW (inset) and high-resolution TEM image of the SiNT (bottom), revealing single-crystalline AuNW and polycrystalline SiNT, respectively.

segments. The NW segment can either be made of a single material or consist of several subsegments of different materials (metals, alloys, or compound semiconductors), while the NT segment can be made from carbon, silicon, or silica; the two end NT segments in NT/NW/NT architectures can be made of the same material or of different materials. These branched hybrid nanoarchitectures, prepared for the first time, suggest potential fabrication of large-scale three-dimensionally interconnected multifunctional nanocircuits, nanodevices, and nanosystems.

Received: April 15, 2009
Published online: June 18, 2009

Keywords: heterojunctions · nanostructures · nanotubes · nanowires · template synthesis

- [1] M. S. Gudiksen, L. J. Lauhon, J. F. Wang, D. C. Smith, C. M. Lieber, *Nature* **2002**, *415*, 617.
- [2] Y. Wu, R. Fan, P. Yang, *Nano Lett.* **2002**, *2*, 83.
- [3] S. R. Nicewarner-Peña, R. G. Freeman, B. D. Reiss, L. He, D. J. Peña, I. D. Walton, R. Cromer, C. D. Keating, M. J. Natan, *Science* **2001**, *294*, 137.
- [4] B. D. Reiss, R. G. Freeman, I. D. Walton, S. M. Norton, P. C. Smith, W. G. Stonas, C. D. Keating, M. J. Natan, *J. Electroanal. Chem.* **2002**, *522*, 95.
- [5] K. B. Lee, S. Park, C. A. Mirkin, *Angew. Chem.* **2004**, *116*, 3110; *Angew. Chem. Int. Ed.* **2004**, *43*, 3048.
- [6] F. Liu, J. Y. Lee, W. J. Zhou, *Small* **2006**, *2*, 121.
- [7] S. Park, J. H. Lim, S. W. Chung, C. A. Mirkin, *Science* **2004**, *303*, 348.
- [8] A. K. Bentley, J. S. Trethewey, A. B. Ellis, W. C. Crone, *Nano Lett.* **2004**, *4*, 487.
- [9] C. Yang, C. J. Barrelet, F. Capasso, C. M. Lieber, *Nano Lett.* **2006**, *6*, 2929.
- [10] Y. Wu, J. Xiang, C. Yang, W. Lu, C. M. Lieber, *Nature* **2004**, *430*, 61.
- [11] S. J. Hurst, E. K. Payne, L. Qin, C. A. Mirkin, *Angew. Chem.* **2006**, *118*, 2738; *Angew. Chem. Int. Ed.* **2006**, *45*, 2672.
- [12] W. Lee, R. Scholz, K. Nielsch, U. A. Gosele, *Angew. Chem.* **2005**, *117*, 6204; *Angew. Chem. Int. Ed.* **2005**, *44*, 6050.
- [13] F. S. Ou, M. M. Shaijumon, L. Ci, D. Benicewicz, R. Vajtai, P. M. Ajayan, *Appl. Phys. Lett.* **2006**, *89*, 243122.
- [14] K. A. Dick, K. Deppert, M. W. Larsson, T. Mårtensson, W. Seifert, L. R. Wallenberg, L. Samuelson, *Nat. Mater.* **2004**, *3*, 380.
- [15] D. L. Wang, F. Qian, C. Yang, Z. H. Zhong, C. M. Lieber, *Nano Lett.* **2004**, *4*, 871.
- [16] J. Li, C. Papadopoulos, J. Xu, *Nature* **1999**, *402*, 253.
- [17] G. W. Meng, Y. J. Jung, A. Cao, R. Vajtai, P. M. Ajayan, *Proc. Natl. Acad. Sci. USA* **2005**, *102*, 7074.
- [18] J. Sha, J. Niu, X. Ma, J. Xu, X. Zhang, Q. Yang, D. Yang, *Adv. Mater.* **2002**, *14*, 1219.
- [19] N. I. Kovtyukhova, T. E. Mallouk, T. S. Mayer, *Adv. Mater.* **2003**, *15*, 780.